VOLUME 36 NUMBER 12

ACCOUNTS of CHEMICAL RESEARCH®

DECEMBER 2003

Scientific Basis for Process and Catalyst Design in the Selective Oxidation of Methane to Formaldehyde

FRANCESCO ARENA* AND ADOLFO PARMALIANA

Dipartimento di Chimica Industriale e Ingegneria dei Materiali, Università degli Studi di Messina, Salita Sperone 31, I-98166 S. Agata (Messina), Italy

Received April 15, 2002

ABSTRACT

The mechanism and kinetics of the gas-phase selective oxidation of methane to formaldehyde (MPO) are revised in the general context of catalytic oxidations. In agreement with ab initio calculations of the energy barrier for the activation of methane on transition metal oxide complexes, a formal Langmuir−Hinshelwood kinetic model is proposed which accounts for the "steady-state" conditions and activity−selectivity pattern of MPO catalysts, providing an original support to process design and catalyst development.

I. Introduction

Catalytic selective oxidations (CSOs) have a strategic importance in modern industrial chemistry, allowing the production of chemicals, monomers, and intermediates, which in turn are used for making numerous finite products, from resins and plastics to paints, solvents, rubbers, drugs, etc. The economic impact of CSOs is considerable and amounted to a world turnover of ca. $50 billion U.S. in 1998.[1]

Almost all CSO processes entail the specific functionalization of "reactive" organic substrates, such as alkenes and aromatics, which today are easily and cheaply obtained from crude oil, by selective oxidation, oxidative dehydrogenation, and oxidative ammonolysis reactions.[1−4] However, market forecasts indicate that, in the medium term, the petrochemical industry will move to a direct use of alkanes as feedstock rather than oil, these being even more economical, readily available, safer, and less toxic than olefins and aromatics.[1−3] This expected breakthrough in the petrochemical industry feedstock supply would be prompted by the worldwide abundance of natural gas (NG) reserves (consisting mainly of C_1−C_4 alkanes) compared to the limited oil reserves which will cause an increase in the price of oil-derived products.[2,3] Consequently, potential process routes employing novel catalytic approaches in combination with low-cost alkane feedstocks would result in significant economic advantages over current technologies and are inevitably destined to rise.[2,3,6−8] Hence, the direct conversion of NG streams, at present almost exclusively used as fuel, to commodity chemical products is researched intensely by both chemical companies and technology licensors. Also, an increasing demand for plastics will make the existing production of light olefins insufficient, and require dedicated processes for the direct production of individual monomers by conventional dehydrogenation or selective oxy-dehydrogenation of the corresponding alkane.[2,3]

Despite many catalysts for the selective oxidation of C_1−C_5 alkanes being proposed in both the scientific and patent literature, the low *productivity* of the processes still remains the main drawback to their industrial exploitation.[2−8] Moreover, while several key aspects of catalyst design are common for the functionalization of C_2−C_5 alkanes, the catalytic partial oxidation of methane to CH_3-

Francesco Arena received his degree in industrial chemistry (1987) and the master's degree in chemical processes technologies (1989) from the University of Messina. After several official post-doctoral fellowships, he became Assistant Professor (1992) and then Associate Professor of Industrial Chemistry and Catalysis (2001) at the University of Messina. His research interest actually focuses on heterogeneous catalytic materials and processes.

Adolfo Parmaliana received his degree in industrial chemistry from the University of Messina (1981). After holding an Associate Professorship in Catalysis at the University of Rome "La Sapienza" (1998−2000), he is currently Full Professor of Industrial Chemistry at the University of Messina. His research interest comprises fundamental and applied heterogeneous catalysis and development of novel catalytic processes.

* Corresponding author. Phone: +39 090 6765606. Fax: +39 090 391518. E-mail: Francesco.Arena@unime.it.

10.1021/ar020064+ CCC: $25.00
Published on Web 09/20/2003

OH and/or HCHO (MPO) cannot be rationalized according to the rules already established for higher hydrocarbons.[1,2,4,5] Because of the low reactivity of the substrate, the mechanistic aspects of the MPO are very peculiar and require ad hoc catalysts, experimental conditions, and reactor technologies to maximize the yield of the desired product(s).[2,4,6−28]

Since the work in the 1980s by Foster[9] and Spencer and Pereira,[10,11] who showed the feasibility of the MPO using MoO_3/SiO_2 and V_2O_5/SiO_2 catalysts, a great deal of research has been focused on various unpromoted or promoted oxide systems and factors controlling their reactivity.[8−30] It has been shown that, as well as a suitable chemical formulation, a necessary prerequisite of MPO catalysts entails the "isolation" of the active sites to prevent the over-oxidation of CH_3OH and/or HCHO to CO_x.[1,2,4−8,15,16,20,24−29,31,38] Dispersion and redox features of the active phase are thus the key factors determining the behavior pattern of MPO catalysts.[7,8,15,16,20−22,24−29]

Although the unique functionality of the silica carrier in driving the MPO was earlier documented,[6−8,10−20] the catalytic performance of silicas depends on the method of preparation, according to the reactivity scale "precipitation > sol−gel > pyrolysis",[6−8,13,17,30] as it determines the density of "strained siloxane bridges", early presumed to be the active sites in MPO.[13,30] In fact, recent studies on the catalytic MPO functionality of silica have shown that *constitutional* iron "impurities" play the role of *active* centers, enabling the redox cycle under reaction conditions.[25−27] Namely, while "isolated" Fe^{3+} species assist selective oxidation paths, leading to CH_3OH/HCHO, aggregate moieties mostly yield CO_x because of a high availability of lattice oxygen, promoting the further oxidation of desired product(s).[1,16,25−27] Because of a relatively high concentration and dispersion of Fe^{III} impurities,[17,25,27] a "precipitated" silica sample (Si 4-5P grade, Akzo product) shows a superior "activity−selectivity" pattern and STY_{HCHO} values larger than those of MoO_3- and V_2O_5-promoted silica catalysts in the range 650−750 °C.[18,23]

In addition to catalyst formulations involving silica as the carrier of transition metal ions (e.g., Mo^{VI}, V^{V}, Fe^{III}, etc.), the effectiveness of stoichiometric compounds such as $Fe_2(MoO_4)_3$ and $FePO_4$ in the partial oxidation of methane to CH_3OH and HCHO has been claimed.[7,31] Detailed investigations of the structure of the active sites have shown that the counteranion in such systems acts as a "spacer", allowing the "isolation" of the Fe^{3+} active centers, thus addressing the basic requirements of FeO_x/SiO_2 catalysts.[7,31]

Besides progress on catalyst optimization, systematic studies on the steady-state gas−solid interactions aimed at elucidating the mechanism and kinetics of the MPO on silica-based catalysts have been reported recently.[32−36] According to the general principles of oxidation catalysis,[1,4,5,37] we have developed a formal kinetic model describing in detail the steady-state conditions and activity−selectivity pattern of silica-based catalysts,[32−35] thus giving a scientific background to catalyst optimization and process design.[24,35]

This Account provides an overview of the fundamental aspects of the MPO reaction on oxide catalysts, emphasizing, in particular, our recent contributions to kinetic modeling and catalyst development.

II. Reaction Mechanism and Kinetics

A. Catalyst "Steady State". It is generally recognized that a comprehensive knowledge of the mechanism and molecular dynamics of a heterogeneous catalytic process can be attained only by a proper physicochemical characterization of the catalyst under real "working" conditions.[1,2,4,5] As the steady-state condition of a catalyst intimately depends on the reaction system, during oxidation reactions both metal and metal oxide catalysts establish a dynamic "equilibrium" with the reaction atmosphere, attaining a peculiar state which involves the concomitant presence of both surface-*reduced* and -*oxidized* sites.[1,4,5,37] In this respect, probing the extent of catalyst reduction/oxidation under steady-state conditions offers a valuable opportunity to shed light onto the reaction mechanism and kinetics of oxidative processes.[1,4,5,37]

Although the origin (*lattice* or *molecular*) of active oxygen species could not be probed unambiguously,[8,13−17,19−22,31] general agreement comes from the fact that MPO reaction proceeds via a surface-assisted redox path involving the cyclic activation of methane and molecular oxygen.[7,8,10−17,20−22,31] Then, carrying out in situ reaction temperature oxygen chemisorption (RTOC) measurements to evaluate the extent of catalysts reduction at the steady state, we found that the activity of various silica samples and "diluted" (≤5 wt %) MoO_3- and V_2O_5-promoted silica catalysts matched with the respective (absolute) "density of reduced sites" (ρ).[17,27] This was preliminary evidence of the fact that the capability to stabilize *reduced sites* is a key factor for the performance of oxide catalysts in MPO.[17] Otsuka and Wang came to analogous conclusions using the in situ XPS analysis of the $FePO_4$ catalyst,[7,31] while an irreversible reduction of the silica-supported $FePO_4$ system was found by Alptekin et al. during MPO.[38]

All of this prompted us to undertake a kinetic−mechanistic study of the MPO reaction, starting from a systematic evaluation of the effects of the reaction mixture composition on the steady state of the "precipitated" Si 4-5P silica catalyst.[32−34]

Varying systematically P_{CH_4} and P_{O_2} in a range corresponding to a P_{CH_4}/P_{O_2} ratio between ca. 0.5 and 8, we found that the "fractional density of reduced sites" (θ_{red}, ρ/ρ_0), as evaluated by RTOC measurements, follows two opposite trends, as shown in Figure 1A. A log plot of these data (Figure 1B) provides in fact two inverse linear relationships, the slope of which indicates a square-root (0.5) and an inverse square-root (−0.5) dependence of θ_{red} on P_{CH_4} and P_{O_2} (e.g., $\theta_{red} \propto \sqrt{P_{CH_4}/P_{O_2}}$), respectively.[32−35] This indicates a "concerted" or "push−pull" redox mechanism involving the same active sites;[1,4,5,32−39] such findings prove that the *redox potential* of the reaction mixture (e.g., P_{CH_4}/P_{O_2}) mostly controls the steady-state condition of the active sites.[1,4,5,37] This means that the activation of meth-

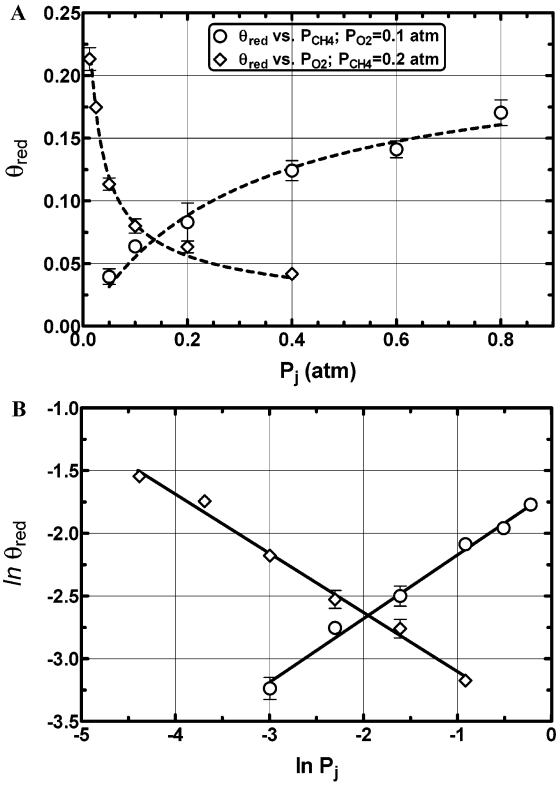

FIGURE 1. (A) Fractional density of reduced sites (θ_{red}) vs P_{CH_4} and P_{O_2} (T_R = 650 °C). (B) Log plot of θ_{red} vs P_{CH_4} and P_{O_2}. [Adapted from ref 34 with permission from the American Institute of Chemical Engineers.]

ane and oxygen molecules proceeds via a *dissociative path* on ensembles of active sites releasing/accepting (at least) two oxygen atoms:[7,26,31,40]

$$CH_4 + 2\rho\text{-}O \rightarrow HCHO + H_2O + 2\rho \quad \text{(i)}$$

$$2\rho + O_2 \rightarrow 2\rho\text{-}O \quad \text{(ii)}$$

Since the active sites of the "precipitated" silica are "isolated" Fe^{3+} species dispersed into the inert SiO_2 matrix,[24−29] the above results show that HCHO formation requires two neighboring $Fe{-}O^{n+}$ centers, enabling a *four-electron-transfer* process.[40] However, also with the hypothesis of one-electron transfer *per* Fe atom, the total concentration of active sites (ρ_0, 373.63 × 10^{-9} $mol_O \cdot g^{-1}$) found on the "precipitated" silica catalyst[32−34] really accounts for an Fe concentration (0.004 wt %) lower by ca. 1 order of magnitude than the nominal iron concentration (0.02−0.03 wt %).[27−29] Evidently, a large fraction of Fe^{3+} ions cannot assist the activation of CH_4, perhaps because of too high dispersion, though the presence of Fe_2O_3 clusters or Fe^{3+} ions incorporated into the silica lattice,[25] resulting in a lower concentration of available active sites than that expected on the basis of the nominal loading, cannot be excluded.

Then, considering that the sum of reduced [$(\rho_0\theta_{red})$] and oxidized [$(\rho_0(1 - \theta_{red})$] sites corresponds to the total number of active sites (ρ_0), the rates of the catalyst reduction by methane (1) and oxidation by molecular

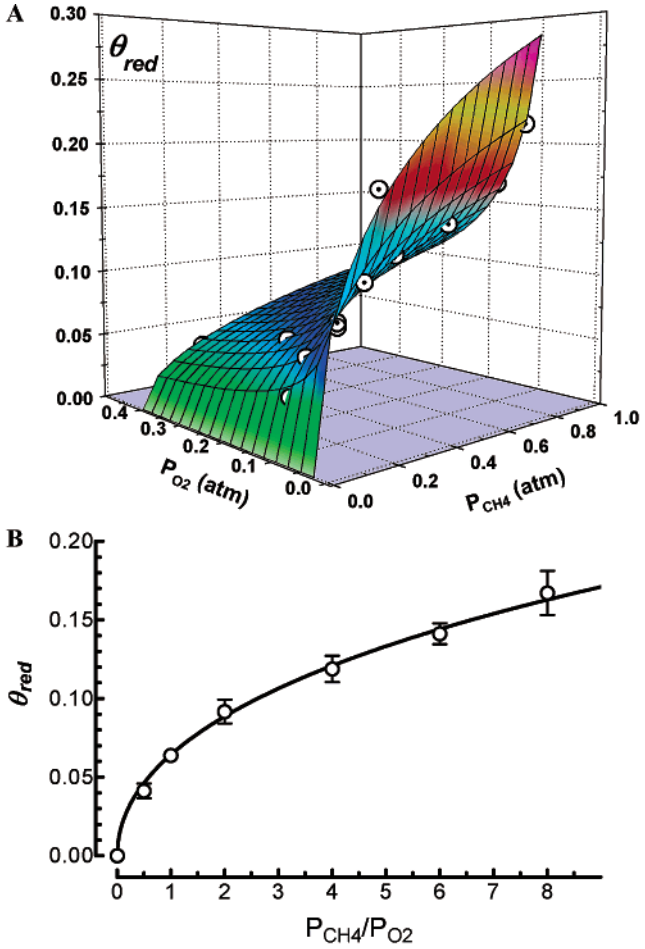

FIGURE 2. (A) 3-D fitting of θ_{red} vs $P_{CH_4} - P_{O_2}$. (B) Curve fitting of θ_{red} vs P_{CH_4}/P_{O_2} (T_R = 650 °C). [Adapted from ref 33 with permission from Elsevier Science.]

oxygen (2) are

$$\text{rate}_{red} = k_{red}P_{CH_4}(\rho_0 - \rho)^2 = k_{red}P_{CH_4}\rho_0^2(1 - \theta_{red})^2 \quad (1)$$

$$\text{rate}_{ox} = k_{ox}P_{O_2}\rho^2 = k_{ox}P_{O_2}\rho_0^2\theta_{red}^2 \quad (2)$$

Considering negligible the relative rate of lattice oxygen ion diffusion through the silica lattice,[4,6,13−17,21,32−34] the mass balance of active sites under steady-state conditions results in the following equation:

$$\theta_{red} = \frac{\sqrt{k_{red}/k_{ox}}(P_{CH_4}/P_{O_2})^{0.5}}{1 + \sqrt{k_{red}/k_{ox}}(P_{CH_4}/P_{O_2})^{0.5}} \quad (3)$$

which describes the fraction of surface reduced sites (θ_{red}) as a function of P_{CH_4} and P_{O_2}. Assuming that the term $[(k_{red}P_{CH_4}/k_{ox}P_{O_2})^{0.5}]$ would be significantly less than unity, the above equation agrees with the experimental dependence of θ_{red} on the square root of the P_{CH_4}/P_{O_2} ratio, giving in fact a very good fitting of RTOC experimental data, as shown in Figure 2. Nonlinear regression analysis of these data by eq 3 gives a value of k_{red}/k_{ox} of 4.73 × 10^{-3}, which really means a rate of catalyst reduction considerably smaller than oxidation, in agreement with the fact that

Table 1. Activation Energy of MPO Elementary Steps

step	surface reactions	E (kJ mol^{-1}) MoO_3/SiO_2[b]	E (kJ mol^{-1}) V_2O_5/SiO_2[b]
1[a]	$CH_4 + 2MeO \leftrightarrows MeOCH_3 + MeOH$	204/282	211/317
2	$MeOCH_3 + MeO \leftrightarrows MeOCH_2 + MeOH$	42/193	13/222
3	$MeOCH_2 \leftrightarrows HCHO + Me$	84/0	126/0
4[a]	$HCHO + MeO \leftrightarrows MeOCH_2O$	31/52	22/62
5[a]	$MeOCH_2O + MeO \leftrightarrows CO + 2MeOH$	124/337	89/288
6	$2MeOH \leftrightarrows H_2O + MeO + Me$	131/0	97/0
7	$2Me + O_2 \leftrightarrows 2MeO$	0/269	0/190
8[a]	$MeOCH_3 + 2MeO \leftrightarrows MeOCH_2OMe + MeOH$	0/179	0/207
9	$MeOCH_2OMe + 2MeO \leftrightarrows CO_2 + 2MeOH + 2Me$	0/271	0/303
10	$MeOCH_3 + MeOH \leftrightarrows CH_3OH + MeO + Me$	106/20	100/25
11[a]	$CO + MeO \leftrightarrows MeCO_2$	180/198	147/231
12	$MeCO_2 \leftrightarrows CO_2 + Me$	124/254	137/240

[a] Steps that are significant under MPO conditions. [b] E values referred to forward/reverse reactions, respectively. [Adapted from ref 12 with permission from the American Institute of Chemical Engineers.]

Table 2. Literature Data on Reaction Order and Apparent Activation Energy of the MPO Reaction

catalyst	T range (°C)	reaction order $[CH_4]$	reaction order $[O_2]$	reaction order [other]	E_{app} (kJ/mol)	ref
1.8 wt % MoO_3/SiO_2	575−650	1	0		189	10
1.3 wt % V_2O_5/SiO_2	500−600	1	0		227	11
bulk $Fe_2(MoO_4)_3$	650−750	1	0.5		290	39
bulk $FePO_4$	575−650	0.66 ± 0.07	0.45 ± 0.05		164 ± 9	38
bulk $FePO_4$	350−400	<1	0		145 ± 5[a]	7
5 wt % $FePO_4/SiO_2$	600−650	0.61 ± 0.07	0.28 ± 0.03		144 ± 4	38
5 wt % $FePO_4/SiO_2$	600−650	0.48 ± 0.05	0.21 ± 0.03	0.23 ± 0.04[a]	155 ± 3	38
2−7 wt % MoO_3/SiO_2	550−800	nd	nd		159−197	20
2−50 wt % V_2O_5/SiO_2	550−700	nd	nd		163−197	20
precipitated SiO_2	650	1.1	0.2		nd	33
precipitated SiO_2	500−800	1.1 ± 0.1	0.2 ± 0.06		159 ± 8	34
precipitated SiO_2	575−625	0.9 ± 0.1	0.3 ± 0.03		142 ± 8	36

[a] In the presence of hydrogen. [b] In the presence of water vapor. nd, not determined.

the activation of the C−H bond generally represents the rate-determining step (rds) of the selective oxidation of light alkanes on oxide catalysts.[1,2,4−8,10−16,20,21,32−37,40]

B. Mechanism and Kinetics. Earlier kinetic studies by Spencer et al. were aimed at modeling the activity−selectivity pattern of MoO_3/SiO_2 and V_2O_5/SiO_2 catalysts through a microkinetic analysis of the elementary reaction steps.[12] From thermodynamic data of intermediates, they calculated the values of activation energies summarized in Table 1,[12] by which they were able to simulate the catalytic pattern of MoO_3/SiO_2 and V_2O_5/SiO_2 systems in agreement with macrokinetic data.[10,11] Namely, the model predicted negligible activation energies for oxygen replenishment and methoxy intermediate oxidation (Table 1), and first showed the essential chemistry of the MPO reaction.[12]

Further attempts to model the kinetics of the MPO reaction on various catalysts were mostly based on experimental relationships in the form of power-law equations,[6−8,20,32−36,38,39] a summary of which is presented in Table 2 in terms of reaction orders and apparent activation energy values. Irrespective of temperature and catalyst composition, these data indicate that the kinetics of the MPO substantially follow pseudo-first- and zero-order kinetics with respect to P_{CH_4} and P_{O_2},[10−12] in particular, fact that MPO catalysts are prevalently in the oxidized state,[17,22] according to the assumption (Table 1) that oxygen incorporation is an easy reaction step.[7−15,20,21,32−34,40] Therefore, the small effect of the oxygen concentration ($n < 0.5$) on reaction rate proves that the activation of the substrate acts as the rds of a reaction network involving "strongly adsorbed" *electrophilic* oxygen species[4] and CH_4 molecules in a slight, if any, interaction with the catalyst surface.[13−15,30,38,39] In fact, in situ FTIR spectroscopy could not reveal the presence of adsorbed C-containing intermediates, and the interaction of methane with the catalyst surface is mainly deduced from theoretical considerations or indirect evidence.[13,14,22,30] Otsuka et al.[39] even inferred a zero-order oxygen dependence for the kinetics of MPO on the $Fe_2(MoO_4)_3$ catalyst and, thus, an Eley−Rideal mechanism from the following experimental rate equation:

$$\text{rate}_{CH_4} = (kP_{CH_4})\frac{\sqrt{[KP_{O_2}]}}{1+\sqrt{[KP_{O_2}]}} \qquad (4)$$

This equation implies no direct influence of the P_{CH_4}/P_{O_2} ratio on the catalytic activity, probably because of the major contribution of lattice oxygen to HCHO formation.[4,5,39] In fact, it entails a zero-order oxygen dependence, provided that $\sqrt{[KP_{O_2}]} \gg 1$, whereas at low oxygen concentration ($\sqrt{[KP_{O_2}]} < 1$) it shifts to a kinetic dependence on P_{O_2} up to 0.5, accounting thus for a lowering in reaction rate under oxygen-lean conditions.[7,31,39] Really, intermediate oxygen reaction orders (0.2−0.3) were experimentally found for $FePO_4$[38] and the "precipitated" Si 4-5P silica catalysts.[32−36]

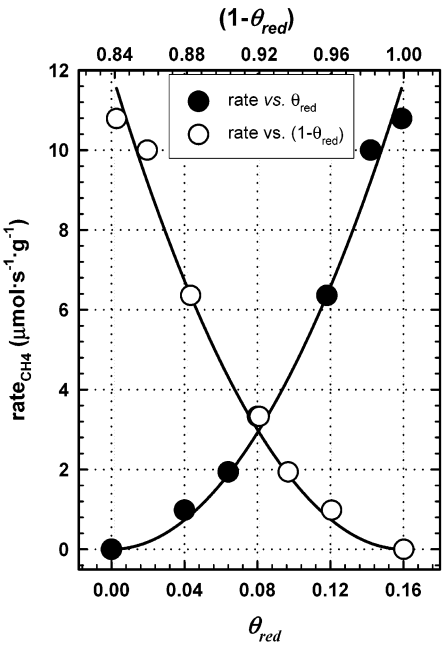

FIGURE 3. Reaction rate vs θ_{red} and $(1 - \theta_{red})$ (T_R = 650 °C). [Adapted from ref 33 with permission from Elsevier Science.]

Then, starting from eq 3 for predicting the steady state of the silica catalyst, we developed a rigorous Langmuir−Hinshelwood-type kinetic model able to rationalize all the above experimental evidence.[31−33] Since previous findings suggest that surface reactions involving catalyst reduction (i) and oxidation (ii) can be considered irreversible,[1,7,8,10−15,22,30−36,39] for the "steady-state" approximation the rate of methane conversion ($rate_{CH_4}$) must equal that of the single steps:

$$rate_{CH_4} = k_{ox}P_{O_2}\rho_0^{\,2}\theta_{red}^{\,2} = k_{red}P_{CH_4}\rho_0^{\,2}(1 - \theta_{red})^2 \quad (5)$$

This relationship entails a second-order dependence of reaction rate on ρ_0,[35] θ_{red} and θ_{ox}, as confirmed by the fitting of experimental data shown in Figure 3.[33,34] Further, substituting expression (3) for θ_{red}, the formal kinetic equation is obtained:

$$rate_{CH_4} = \rho_0^{\,2}\frac{k_{red}P_{CH_4}}{\left(1 + \sqrt{\frac{k_{red}P_{CH_4}}{k_{ox}P_{O_2}}}\right)^2} \quad (6)$$

which provides a very good fitting of reaction rate data (T_R, 650 °C) with varying P_{CH_4} and P_{O_2}, as shown in Figure 4. This equation describes the kinetic model of selective oxidations proceeding by a redox mechanism without a contribution of lattice oxygen.[1,4,5,32−37] It predicts a rate close to zero in the absence of gas-phase oxygen ($P_{CH_4}/P_{O_2} \rightarrow \infty$),[7,8,16,17,21,39] probing that as the P_{CH_4}/P_{O_2} ratio rises the reaction order on P_{CH_4} becomes lower than 1, as a consequence of a steady decrease in the concentration of (oxidized) active sites prompting CH_4 conversion.[1,4,7,32−36,39]

Starting from this kinetic model, McCormick and coworkers developed further relationships to account for the

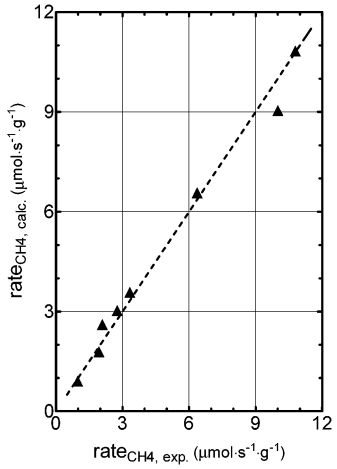

FIGURE 4. Calculated vs experimental reaction rate values (T_R = 650 °C). [Adapted from ref 33 with permission from Elsevier Science.]

effects of the product selectivity on the catalyst steady state,[36] coming to the conclusion that the stationary condition of the catalyst might be greatly affected by the sequential surface reactions of HCHO and CO, especially at high levels of CH_4 conversion.[34−36] However, an "ideal" batch reactor operating at differential conversion (<0.1%) *per* pass, then with very slight changes in product selectivity, has been used throughout our kinetic evaluations.[17,32−34] In other words, both kinetic and RTOC measurements were carried out at rather low contact times to ensure differential conversion levels and limit the occurrence of consecutive oxidation reactions which could seriously affect the steady state of the catalyst.[32−34] In fact, assuming an unchanged product selectivity (S_{HCHO}, 0.75; S_{CO}, 0.19; S_{CO_2}, 0.06), which means a constant CH_4/O_2 stoichiometric reaction coefficient (e.g., n = 1.155),[34] the following integral kinetic equation is obtained from (6):

$$\ln\frac{P_{CH_4,in}}{P_{CH_4}} + \frac{k_{red}}{k_{ox}}\ln\frac{(P_{CH_4,in} - a/n)}{(P_{CH_4} - a/n)} + 2\sqrt{\frac{k_{red}}{k_{ox}}} \times \ln\frac{[(P_{CH_4,in} - a/2b) + \sqrt{(P_{CH_4,in} - a/2n)^2 - a^2/4n^2}]}{[(P_{CH_4} - a/2n) + \sqrt{(P_{CH_4} - a/2n)^2 - a^2/4n^2}]} = (\rho_0^{\,2}k_{red})\lambda t \quad (7)$$

where $a = (nP_{CH_4,in} - P_{O_2,in})$, $n = (P_{CH_4,in}/P_{O_2,in})$, and λ = 1.06 $mol_{CH_4}\cdot atm_{CH_4}^{-1}\cdot g_{cat}^{-1}$ are constants.[34] Taking into account any changes in reaction mixture composition and its effect on the catalyst steady state,[34] this equation gives a very good fit of integral "batch reactor" data, as shown in Figure 5. Namely, a maximum distance between predicted and experimental values as high as 5−6% in the whole range of CH_4 (0−43%) and O_2 (0−99%) conversion can be observed, whereas the first-order kinetic law shows its limit in accounting for the slowing down in reaction rate caused by the progressive decrease in P_{O_2}, reflected in an extensive reduction of the catalyst surface.[34]

The data reported in Table 2 show that, besides reaction orders, a good agreement also concerns apparent activation energy values. With the exception of the Fe_2-

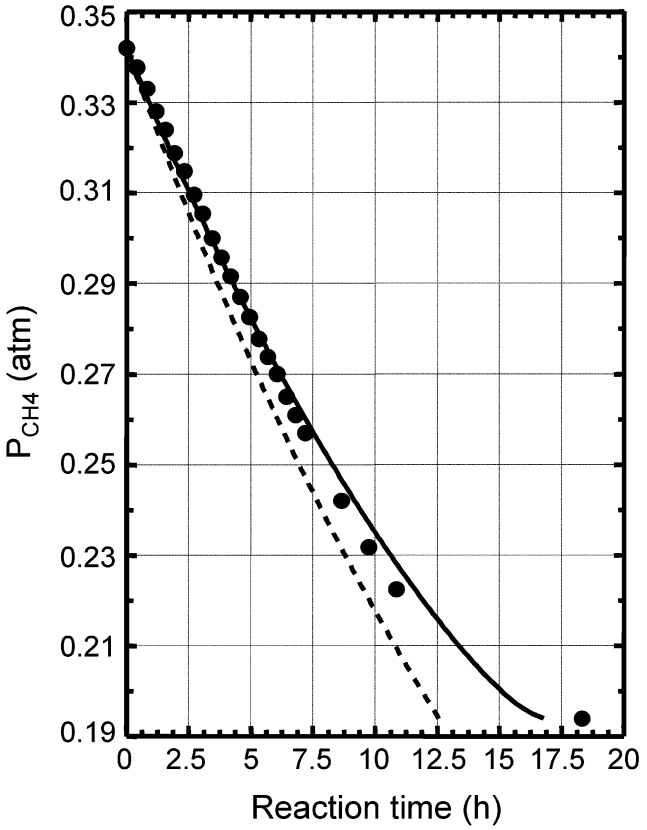

FIGURE 5. Fitting of integral conversion data (T_R = 650 °C; P_{CH_4}/P_{O_2} = 2) by a first-order law (- - -) and model equation (7) (—). [Adapted from ref 34 with permission from the American Institute of Chemical Engineers.]

$(MoO_4)_2$ system, the only one featuring, however, a peculiar major contribution of lattice oxygen which is a strongly temperature activated process (E_{app}, 290 kJ/mol),[39] the E_{app} values are rather comparable (150−200 kJ/mol), and an average value of 140−160 kJ/mol can be reasonably assumed for Fe-based catalysts.[7,8,20,34,36,38] Such an E_{app} value results in very good agreement with the ab initio calculation of the energy barrier (130 kJ/mol) of the activation of CH_4 on the FeO^+ complex, and in particular for the rearrangement of the "$O-Fe^+-(CH_4)$" reactant complex to "$HO-Fe^+-CH_3$" via a transition state (TS1) on the sextet surface of the FeO^+ complex.[40] Although the activation energy value results are rather small compared to the C−H bond energy in methane of 438 kJ/mol,[1,4,40] the energy gap to the formation of the TS1 complex via C−H bond cleavage would be overcome by significant orbital interactions in the reactant complex.[40] Accordingly, the computed energies led the authors to believe that the conversion of methane by late transition metal oxide ions must preferably occur via the following *concerted mechanism*:

$$MO^+ + CH_4 \rightarrow OM^+(CH_4) \xrightarrow{[TS1]}$$
$$HO - M^+ - CH_3 \xrightarrow{[TS2]} M^+(CH_3OH) \rightarrow M^+ + CH_3OH$$

Though based on a simplified reaction scheme, our mechanistic−kinetic model matches both theoretical and experimental findings of the MPO reaction on silica-promoted oxide catalysts, highlighting also some fundamental relationships for the activation energy of reaction steps.[34] Namely, model-predicted values, compared with experimental data in Table 3,[34] confirm that the apparent activation energy of the MPO (E_{app}, 142 ± 8 kJ/mol) stems from the energy barrier of the surface reaction of a methane molecule with (two) oxidized active sites to yield a HCHO molecule and (two) surface-reduced sites (E_{red}, 159 ± 8 kJ/mol). On the other hand, with an E_{ox} value of ca. 20 kJ/mol, the model conveys that the O_2 replenishment is a nonactivated reaction step and that CH_4 activation controls the overall reaction kinetics.[12,32−34,39] In fact, using the above data for calculating the values of the kinetic constants at various T in the range 500−800 °C,[34] an excellent fit of reaction rate values of the "precipitated" silica catalyst under different experimental conditions (e.g., T, P_{CH_4}, P_{O_2}, P_{tot}/F_{tot}) is obtained by the rate equation (6), as shown in Figure 6.

Table 3. Activation Energy of Surface Reactions: Model vs Experimental Data

reaction step	E notation	model value	exptl value (kJ mol^{-1})
$CH_4 + O_2 \rightarrow HCHO + H_2O$	E_{app}	$\cong E_{red}$	142 ± 8
$CH_4 + 2\rho\text{-}O \rightarrow HCHO + H_2O + 2\rho$	E_{red}	E_{red}[a]	159 ± 8
$2\rho + O_2 \rightarrow 2\rho\text{-}O$	E_{ox}	−	20 ± 10

[Adapted from ref 34 with permission from the American Institute of Chemical Engineers.]

The above kinetic model, fully based on RTOC characterization data of the catalyst at the "steady state",[32−34] has been further handled to derive basic relationships to predict the activity−selectivity pattern of the "precipitated" silica catalyst.[35]

Expressing the methane conversion as the ratio of reaction ($rate_{CH_4}$) and feeding (F_{CH_4}) rates,

$$X_{CH_4} = \frac{k_{red} P_{CH_4} \rho_0^2 (1 - \theta_{red})^2}{F_{CH_4}} \qquad (8)$$

and considering that $P_{CH_4} = P_{tot}\chi_{CH_4}$ and $F_{CH_4} = F_{tot}\chi_{CH_4}$, eq 8 becomes

$$X_{CH_4} = \frac{P_{tot}}{F_{tot}} k_{red} \rho_0^2 (1 - \theta_{red})^2 = \frac{P_{tot}}{F_{tot}} k_{red} \rho_0^2 \frac{1}{\left(1 + \sqrt{\frac{k_{red}}{k_{ox}} \frac{P_{CH_4}}{P_{O_2}}}\right)^2} \qquad (9)$$

This relationship indicates that, at a given T, the level of *methane conversion* can be properly tuned by the *experimental factors* P_{tot}/F_{tot} and P_{CH_4}/P_{O_2}, since the other parameters depend on the properties of the solid.[35]

Moreover, taking into account a low affinity of MPO catalysts for CO_2 formation, and considering the stoichiometry (1:1) of the surface reaction between HCHO and oxidized sites to form CO,[12,13,32−34,36,39] with the related kinetic constant being k_{red}', the integral expressions for

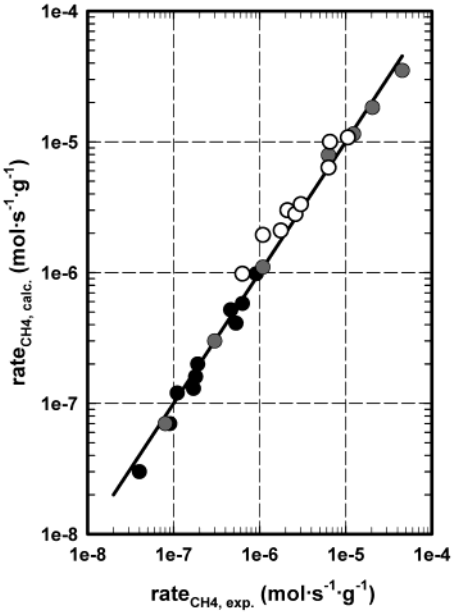

FIGURE 6. Calculated vs experimental reaction rate values at different P_{CH_4}, P_{O_2}, and T. [Adapted from ref 34 with permission from the American Institute of Chemical Engineers.]

HCHO selectivity (S_{HCHO}) with contact time (P_{tot}/F_{tot}),

$$S_{HCHO} = \frac{k_{red}\rho_0(1-\theta_{red})}{[k_{red}' - k_{red}\rho_0(1-\theta_{red})]} \times \frac{(e^{-k_{red}\rho_0^2(1-\theta_{red})^2(P_{tot}/F_{tot})} - e^{-k_{red}'\rho_0(1-\theta_{red})(P_{tot}/F_{tot})})}{(1 - e^{-k_{red}\rho_0^2(1-\theta_{red})^2(P_{tot}/F_{tot})})} \quad (10)$$

and CH_4 conversion (X_{CH_4})

$$S_{HCHO} = \frac{k_{red}\rho_0(1-\theta_{red})}{[k_{red}' - k_{red}\rho_0(1-\theta_{red})]} \times \frac{(e^{-X_{CH4}} - e^{-[k_{red}'/k_{red}\rho_0(1-\theta_{red})]X_{CH4}})}{(1 - e^{-X_{CH4}})} \quad (11)$$

were obtained from the analogy between a catalyst bed and a homogeneous "batch" reaction system, provided that contact time (e.g., P_{tot}/F_{tot}) is used instead of absolute time.[35] Once again, the predictions of model equations (9), (10), and (11) are in excellent agreement with experimental "X_{CH_4}–S_{HCHO} vs P_{tot}/F_{tot}" (A) and "S_{HCHO} vs X_{CH_4}" (B) data (T, 650 °C), as shown in Figure 7,[35] and provide the first mathematical description of the effect of contact time on methane conversion and formaldehyde selectivity.[6–21]

III. Catalyst Requirements and Development

It is generally accepted that reducibility under reaction conditions, nature, density, and heterogeneity of active sites together determine the behavior pattern of oxide catalysts in selective oxidations.[1,4,5] Nevertheless, a general outline of the requirements of MPO catalysts is a rather complicated task, as reactivity of the substrate, reaction conditions, and catalyst requirements are in turn interrelated.[1,4,5] However, because of the low reactivity of CH_4 molecules and the consequent high temperature needed for methane activation,[1,4,5] experimental results suggest that a proper design of MPO catalysts must ensure a rather high dispersion of a suitable transition metal oxide phase over an "inert" matrix featuring a medium-weak Brönsted acidity.[4–8,10–29]

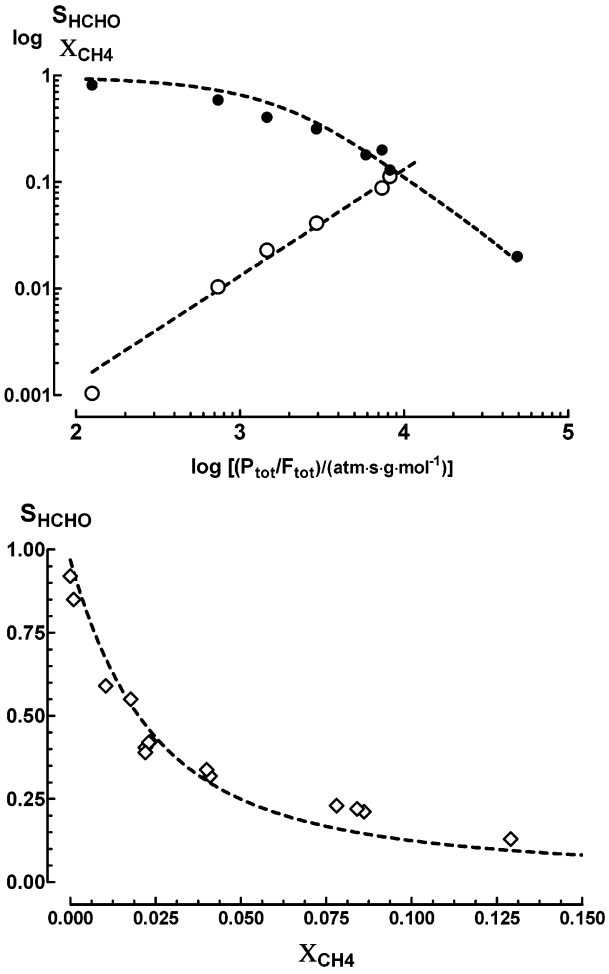

FIGURE 7. (A) Theoretic curves and experimental S_{HCHO} (●) and X_{CH_4} (○) data vs P_{tot}/F_{tot}. (B) Theoretic curve and experimental S_{HCHO} vs X_{CH_4} data (T_R = 650 °C). [Adapted from ref 35 with permission from Elsevier Science USA.]

In fact, attempting to ascertain the structure of Fe^{III} centers for the selective oxidation of CH_4 in the iron phosphate catalyst,[7,31,39] Otsuka et al. concluded that the active sites are *tetrahedrally coordinated* (T_d) Fe^{3+} ions, isolated from each other by the phosphate groups, that act as proton donors for methanol formation via the methoxy intermediate.[31] Analogous conclusions were recently obtained for the Fe-promoted silica catalysts,[16,24–29] the peculiar MPO functionality of silica carriers being ascribable to *highly dispersed* Fe "impurities" in a T_d-like coordination.[18,20,21,23,25,27] Hence, a "high" concentration and dispersion of Fe^{3+} ions looked thus to be essential features which could allow some progress toward the optimization of FeO_x/SiO_2 catalysts.[16,25,27,35]

Considering the limits of conventional preparation methods in ensuring a proper dispersion of the active phase,[25,27] all of these results have prompted our research

Table 4. List of SiO_2 and FeO_x/SiO_2 Catalysts

code	SiO_2 support	preparation method	Fe loading (wt %)	SA_{BET} ($m^2\ g^{-1}$)
Si 4-5P			0.03	380
F5			0.02	607
1-FS	F5	INC/WET	0.10	593
2-FS	Si 4-5P	INC/WET	0.10	402
3-FS	Si 4-5P	INC/WET	0.43	398
FS-1	Si 4-5P	ADS/PRC	0.35	399
FS-2	F5	ADS/PRC	0.09	601
FS-3	F5	ADS/PRC	0.37	597

[Adapted from ref 28 with permission from Kluwer Academic/Plenum Publishers.]

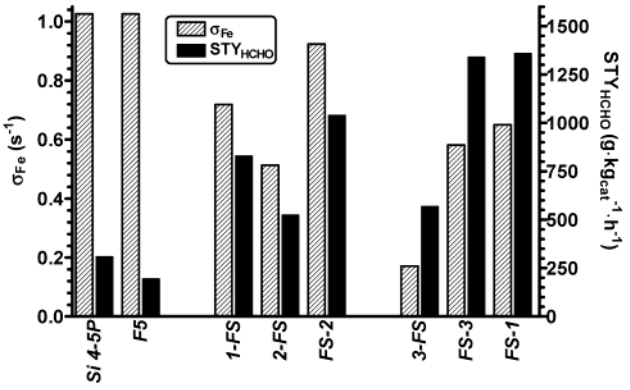

FIGURE 8. Fe specific activity (σ_{Fe}) and STY_{HCHO} for silica and FeO_x/SiO_2 catalysts (T_R = 650 °C). [Adapted from ref 28 with permission from Kluwer Academic/Plenum Publishers.]

group to find an alternative preparation route involving the "adsorption−precipitation" of Fe^{2+} ions (ADS/PRC) on the silica carrier under controlled anaerobic conditions.[24,28,29] Preventing the unavoidable formation of the insoluble Fe^{III} hydroxide (K_{ps}, 10^{-38}), the ADS/PRC route ensures a "selective" interaction of negatively charged hydroxyl groups of the silica surface (pH > 5) with Fe^{2+} ions, resulting in an excellent dispersion of the active phase further to calcination.[24,28,29] Then, FeO_x/SiO_2 systems with different Fe loadings were prepared by ADS/PRC (FS-x), and their catalytic behavior has been compared with those of "conventional" FeO_x/SiO_2 catalysts obtained by incipient wetness (INC/WET) of Si 4-5P and F5 silica samples with aqueous solutions of iron nitrate (x-FS).[28,29]

The list of ADS/PRC and INC/WET catalysts is given in Table 4, while batch reactor activity data of the various systems are compared in Figure 8 in terms of STY_{HCHO} and specific activity of Fe atoms (σ_{Fe}, s^{-1}), calculated on the basis of the analytical Fe loading.[28,29]

Although FeO_x always acts as a promoter of whatever silica carrier is used, it clearly emerges that the ADS/PRC method confers a considerably superior performance to FeO_x/SiO_2 catalysts with respect to the INC/WET route, irrespective of preparation method and total surface area.[24,28,29]

Under standard testing conditions (T = 650 °C; F = 1.0 $L\cdot min^{-1}$ (STP); P_{CH_4}/P_{O_2} = 2; w_{cat} = 0.05 g), Si 4-5P and F5 silica carriers, characterized by the lowest Fe loadings (0.02−0.03 wt %) and expectedly by the highest FeO_x dispersion,[27−29] exhibit an analogous maximum σ_{Fe} of 1.0 s^{-1} and STY_{HCHO} values of ca. 300 and 200 $g\cdot kg_{cat}^{-1}\cdot h^{-1}$, respectively.[24,28,29] Because of a minor dispersion of the active phase, σ_{Fe} values of supported FeO_x/SiO_2 catalysts are always lower than 1.0 s^{-1}, while the STY_{HCHO} values (Figure 8) are generally higher.[24,28,29]

At lower Fe loading (ca. 0.1%), the σ_{Fe} of the 1-FS and 2-FS catalysts (INC/WET) drops to 0.70 and 0.50 s^{-1}, respectively, while the FS-2 sample (ADS/PRC) features a σ_{Fe} very close to that of silicas (0.90 s^{-1}), attaining a STY_{HCHO} of ca. 1000 $g\cdot kg_{cat}^{-1}\cdot h^{-1}$, thus higher by ca. 25% than that of the homologous 1-FS sample.[24,28,29] The different efficiency of the adopted preparation methods, however, becomes even more evident with increasing Fe loading. Indeed, the 3-FS sample (INC/WET) presents a σ_{Fe} of only 0.17 s^{-1}, coupled to a modest STY_{HCHO} of ca. 600 $g\cdot kg_{cat}^{-1}\cdot h^{-1}$, whereas the counterpart FS-1 and FS-3 catalysts (ADS/PRC) feature σ_{Fe} values of 0.60−0.70 s^{-1} and maximum STY_{HCHO} values of ca. 1300 $g\cdot kg_{cat}^{-1}\cdot h^{-1}$.

A more reliable comparison of the catalytic performance of the FS-3 and 3-FS systems can be made by taking into account the results of a catalytic test run on the former sample at a lower contact time (w_{cat} = 0.005 g), thus ensuring a conversion per pass (<0.1%) comparable with that of the counterpart 3-FS. In the absence of any kinetic constraint, the σ_{Fe} of the FS-3 catalyst rises to 0.77 s^{-1} which, coupled to an S_{HCHO} of 55%, results in the remarkable STY_{HCHO} of ca. 3000 $g\cdot kg_{cat}^{-1}\cdot h^{-1}$.

It is noteworthy that this figure is 5 times larger than that of the homologous 3-FS sample, 1 order of magnitude greater than that of "precipitated" silica carrier, and would represent a step forward in potential exploitation of the MPO reaction.[24,28,29]

IV. Conclusions

The mechanism and kinetics of the catalytic selective oxidation of methane to oxygenates on promoted and unpromoted oxide systems have been critically reviewed, leading to the following general conclusions:

(1) The MPO proceeds via a *concerted* redox mechanism involving the activation of the C−H bond of methane by surface electrophilic oxygen species. The redox cycle stabilizes the catalyst surface in a partially reduced form, prompting an easy activation of molecular oxygen.

(2) The density of reduced sites under steady-state conditions depends on the square root of the P_{CH_4}/P_{O_2} ratio, indicating a dissociative activation path of both the CH_4 and O_2 molecules.

(3) The *rate-limiting step* of the MPO reaction on silica is the activation of the C−H bond of methane, the O_2 replenishment being a *nonactivated* reaction step.

(4) In situ characterization of the silica catalyst by RTOC has allowed the development of a formal Langmuir−Hinshelwood model that predicts both the "steady-state" conditions of the catalyst surface and the reaction kinetics.

(5) Tailoring the active phase in the form of "isolated" sites on an inert matrix is a necessary requirement of MPO catalysts. A preparation method based on the "adsorption/precipitation" of Fe^{II} ions on silica, resulting in very effective FeO_x/SiO_2 catalysts, is outlined.

(6) It is hoped that the elucidation of reaction mechanism, kinetics, and catalyst requirements will allow further advances toward an industrial application of the MPO reaction as a viable route for NG oxy-functionalization.

Prof. David G. Lister (D.C.I.I.M., UNIME) is gratefully acknowledged for helpful suggestions and contribution to the final English style of the present Account.

References

(1) Hodnett, B. K. *Heterogeneous Catalytic Oxidation*; J. Wiley & Sons: Ltd.: New York, 2000.

(2) Albonetti, S.; Cavani, F.; Trifirò, F. Key Aspects of Catalyst Design for the Selective Oxidation of Paraffins. *Catal. Rev.-Sci. Eng.* **1996**, *38*(4), 413−438.

(3) Chemical News and Intelligence 2000, Alkane-Activation: Petrochemical Feedstocks of the Future, Chem Systems Ed. (http://www.chemsystems.com/search/docs/abstracts/MC-ALKANE-Absr1.pdf).

(4) Bielañski, A.; Haber, J. *Oxygen in Catalysis*; Marcel Dekker: New York, 1991.

(5) Sokolovskii, V. Principles of Oxidative Catalysis on Solid Oxides. *Catal. Rev.-Sci. Eng.* **1990**, *32*, 1−47.

(6) Brown, M. J.; Parkyns, N. D. Progress in the Partial Oxidation of Methane to Methanol and Formaldehyde. *Catal. Today* **1991**, *8*, 305−335.

(7) Otsuka, K.; Wang, Y. Direct Conversion of Methane into Oxygenates. *Appl. Catal. A* **2001**, *222*, 145−161.

(8) Tabata, K.; Teng, Y.; Takemoto, T.; Suzuki, E.; Bañares, M. A.; Peña, M. A.; Fierro, J. L. G. Activation of Methane by Oxygen and Nitrogen Oxides. *Catal. Rev.-Sci. Eng.* **2002**, *44* (1), 1−58.

(9) Foster, N. R. Direct Catalytic Oxidation of Methane to Methanol. *Appl. Catal.* **1985**, *85*, 1−9.

(10) Spencer, N. D.; Pereira, C. J. Partial Oxidation of CH_4 to HCHO over a MoO_3−SiO_2 Catalyst: A Kinetic Study. *AIChE J.* **1987**, *33*, 1808−1812.

(11) Spencer, N. D.; Pereira, C. J. V_2O_5−SiO_2-Catalyzed Methane Partial Oxidation with Molecular Oxygen. *J. Catal.* **1989**, *116*, 399−406.

(12) Amiridis, M. D.; Rekoske, J. E.; Dumesic, J. A.; Rudd, D. F.; Spencer, N. D.; Pereira, C. J. Simulation of Methane Partial Oxidation over Silica-Supported MoO_3 and V_2O_5. *AIChE J.* **1991**, *37*, 87−97.

(13) Sun, Q.; Herman, R. G.; Klier, K. Selective Oxidation of Methane with Air over Silica Catalysts. *Catal. Lett.* **1992**, *16*, 251−261.

(14) Koranne, M. M.; Goodwin, J. G.; Marcelin, G. Carbon Pathways for the Partial Oxidation of Methane. *J. Phys. Chem.* **1993**, *97*, 673−678.

(15) Koranne, M. M.; Goodwin, J. G.; Marcelin, G. Oxygen Involvement in the Partial Oxidation of Methane on Supported and Unsupported V_2O_5. *J. Catal.* **1994**, *148*, 378−387.

(16) Kobayashi, T.; Nakagawa, K.; Tabata, K.; Haruta, M. Partial Oxidation of Methane over Silica Promoted by 3d Transition Metal Ions. *J. Chem. Soc., Chem. Commun.* **1994**, 1609−1610.

(17) Parmaliana, A.; Sokolovskii, V.; Miceli, D.; Arena, F.; Giordano, N. On the Nature of the Catalytic Activity of Silica-Based Oxide Catalysts in the Partial Oxidation of Methane to Formaldehyde with O_2. *J. Catal.* **1994**, *148*, 514−523.

(18) Arena, F.; Frusteri, F.; Parmaliana, A.; Giordano, N. Temperature Programmed Reaction: A Powerful and Reliable Method for Catalyst Testing in the Partial Oxidation of Methane to Formaldehyde. *Appl. Catal. A* **1995**, *125*, 39−59.

(19) Herman, R. G.; Sun, Q.; Shi, C.; Klier, K.; Wang, C.-B.; Hu, W.; Wachs, I. E.; Bhasin, M. M. Development of Active Oxide Catalysts for the Direct Oxidation of Methane to Formaldehyde. *Catal. Today* **1997**, *37*, 1−14.

(20) Parmaliana, A.; Arena, F. Working Mechanism of Oxide Catalysts in the Partial Oxidation of Methane to Formaldehyde. *J. Catal.* **1997**, *167*, 57−65.

(21) Arena, F.; Giordano, N.; Parmaliana, A. Working Mechanism of Oxide Catalysts in the Partial Oxidation of Methane to Formaldehdye. *J. Catal.* **1997**, *167*, 66−76.

(22) Sun, Q.; Jehng, J.-M.; Hu, H.; Herman, R. G.; Wachs, I. E.; Klier, K. In Situ Raman Spectroscopy during the Partial Oxidation of Methane to Formaldehyde over Supported Vanadium Oxide Catalysts. *J. Catal.* **1997**, *165*, 91−101.

(23) Parmaliana, A.; Arena, F.; Frusteri, F.; Mondello, N. High Yields in the Catalytic Partial Oxidazion of Natural Gas to Formaldehyde: Catalyst Development and Reactor Configuration. *Stud. Surf. Sci. Catal.* **1998**, *119*, 551−556.

(24) Parmaliana, A.; Arena, F.; Frusteri, F.; Mezzapica. A. Fe-doped Silica Catalysts for the Partial Oxidation of Methane to Formaldehyde with Oxygen. German Patent GEM 17-(SÜD CHEMIE AG), 2000.

(25) Arena, F.; Frusteri, F.; Fierro, J. L. G.; Parmaliana, A. Partial Oxidation of Methane to Formaldehyde on Fe-doped Silica Catalysts. *Stud. Surf. Sci. Catal.* **2001**, *136*, 531−536.

(26) Kobayashi T. Selective Oxidation of Light Alkanes over Silica Catalysts Supporting Mononuclear Active Sites−Acrolein Formation from Ethane. *Catal. Today* **2001**, *71*, 69−76.

(27) Parmaliana, A.; Arena, F.; Frusteri, F.; Martinez-Arias, A.; Lopez-Granados, M.; Fierro, J. L. G. Effect of Fe-Addition on the Catalytic Activity of Silicas in the Partial Oxidation of Methane to Formaldehyde. *Appl. Catal. A* **2002**, *202*, 163−174.

(28) Arena, F.; Frusteri, F.; Torre, T.; Venuto, A.; Mezzapica, A.; Parmaliana, A. Tailoring Effective FeO_x/SiO_2 Catalysts in Methane to Formaldehyde Partial Oxidation. *Catal. Lett.* **2002**, *80*, 69−72.

(29) Arena, F.; Frusteri, F.; Spadaro, L.; Venuto, A.; Parmaliana, A. Design, Preparation and Testing of Effective FeO_x/SiO_2 Catalysts in Methane to Formaldehyde Selective Oxidation. *Stud. Surf. Sci. Catal.* **2002**, *143*, 1097−1104.

(30) Vikulov, K.; Martra, G.; Coluccia, S.; Miceli, D.; Arena, F.; Parmaliana A.; Paukshtis, E. FTIR Spectroscopic Investigation of the Active Sites on Different Types of Silica Catalysts for Methane Partial Oxidation to Formaldehyde. *Catal. Lett.* **1996**, *37*, 235−239.

(31) Wang, Y.; Otsuka, K. Structure of Catalytic Active Site for Oxidation of Methane to Methanol by H_2−O_2 Gas Mixture over Iron-Containing Catalysts. *J. Mol. Catal. A* **1996**, *111*, 341−356.

(32) Arena, F.; Frusteri, F.; Parmaliana, A. Modelling the Partial Oxidation of Methane to Formaldehyde on Silica Catalyst. *Appl. Catal. A* **2000**, *197*, 239−247.

(33) Arena, F.; Frusteri, F.; Mezzapica, A.; Parmaliana, A. Kinetic and Mechanistic Study of the Partial Oxidation of Methane to Formaldehyde on Silica Catalysts. *Stud. Surf. Sci. Catal.* **2000**, *130*, 3585−3590.

(34) Arena, F.; Frusteri, F.; Parmaliana, A. Kinetics of the Partial Oxidation of Methane to Formaldehyde on Silica Catalyst. *AIChE J.* **2000**, *46*, 2285−2294.

(35) Arena, F.; Frusteri, F.; Parmaliana, A. Partial Oxidation of Methane to Formaldehyde. A Theoretic−Experimental Approach to Process Design and Catalyst Development. *J. Catal.* **2002**, *207*, 232−236.

(36) McCormick, R. L.; Al Sahali, M. B.; Alptekin, G. O.; Partial Oxidation of Methane, Methanol, Formaldehyde, and Carbon Monoxide over silica: Global Reaction Kinetics. *Appl. Catal. A* **2002**, *226*, 129−138.

(37) Kung, H. H. Kinetic Analysis of a Generalized Catalytic Selective Oxidation Reaction. *J. Catal.* **1992**, *134*, 691−701.

(38) Alptekin, G. O.; Herring, A. M.; Williamson, D. L.; Ohno, T. R.; McCormick, R. L. Methane Partial Oxidation by Unsupported and Silica Supported Iron Phosphate Catalysts. *J. Catal.* **1999**, *181*, 104−116.

(39) Otsuka, K.; Wang, Y.; Yamanaka, I.; Morikawa, A. Kinetic Study of the Partial Oxidation of Methane over $Fe_2(MoO_4)_3$ Catalyst. *J. Chem. Soc., Faraday Trans* **1993**, *89*, 4225−4230.

(40) Yoshizawa, K.; Shiota, Y.; Yamabe, T. Methane-Methanol Conversion by MnO^+, FeO^+, and CoO^+: A Theoretical Study of Catalytic Selectivity. *J. Am. Chem. Soc.* **1998**, *120*, 564−572.

AR020064+